THE JOURNAL OF BIOLOGICAL CHEMISTRY
Vol. 274, No. 38, Issue of September 17, pp. 27237–27243, 1999

Printed in U.S.A.

Expression, Purification, and Functional Analysis of Murine Ectodomain Fragments of CD8$\alpha\alpha$ and CD8$\alpha\beta$ Dimers*

(Received for publication, March 23, 1999, and in revised form, July 6, 1999)

Petra Kern‡, Rebecca E. Hussey, Rebecca Spoerl, Ellis L. Reinherz, and Hsiu-Ching Chang§

From the Laboratory of Immunobiology, Dana-Farber Cancer Institute and Department of Medicine, Harvard Medical School, Boston, Massachusetts 02115

Soluble mouse CD8$\alpha\alpha$ and CD8$\alpha\beta$ dimers corresponding to the paired ectodomains (CD8$_f$) or their respective component Ig-like domains (CD8) were expressed in Chinese hamster ovary cells or the glycosylation variant Lec3.2.8.1 cells as secreted proteins using a leucine zipper strategy. The affinity of CD8$\alpha\alpha_f$ for H-2K^b as measured by BIAcore revealed a ~65 μM K_d, similar to that of CD8$\alpha\beta_f$. Consistent with this result, CD8$\alpha\alpha_f$ as well as CD8$\alpha\beta_f$ blocked the effector function of N15 T cell receptor transgenic cytolytic T cells in a comparable, dose-dependent fashion. Furthermore, both Lec3.2.8.1-produced and Chinese hamster ovary-produced CD8 homodimers and heterodimers were active in the inhibition assay. These results suggest that the Ig-like domains of CD8 molecules are themselves sufficient to block the requisite transmembrane CD8-pMHC interaction between cytolytic T lymphocytes and target cells. Moreover, given the similarities in co-receptor affinities for pMHC, the findings suggest that the greater efficiency of CD8$\alpha\beta$ *versus* CD8$\alpha\alpha$ co-receptor function on T cells is linked to differences within their membrane-bound stalk regions and/or intracellular segments. As recently shown for sCD8$\alpha\alpha$, the yield, purity and homogeneity of the deglycosylated protein resulting from this expression system is sufficient for crystallization and x-ray diffraction at atomic resolution.

CD8 has been shown to function in mediating signal transduction and adhesion on a subset of cells within the T cell compartment and is critically involved in the development of T cells expressing MHC class I-restricted T cell receptor (TCR)[1] (1). CD8 is encoded by two distinct genes, termed CD8α (or Lyt 2) and CD8β (or Lyt 3) and expressed on the cell surface as a mixture of disulfide-linked CD8$\alpha\alpha$ homodimers and CD8$\alpha\beta$ heterodimers (2–7). CD8α is a 34–37-kDa transmembrane glycoprotein whose extracellular segment contains a compact 122-amino acid (aa) N-terminal Ig-like domain and an extended 48-residue stalk region. A 28-aa cytoplasmic domain, including a cysteine motif responsible for interaction with p56^{lck}, follows a canonical hydrophobic transmembrane anchor. CD8β is a 32-kDa glycoprotein sharing a similar architecture as CD8α but with <20% sequence identity (4, 5). The stalk regions of the CD8α and β chains are quite different in length, with the CD8β stalk being 10–13 residues shorter than that of CD8α. Interestingly, the sialic acid content of *O*-linked glycans adducted to CD8β selectively decreases on thymocytes and activated T cells compared with that found on resting T cells. For its cell surface expression, CD8β requires association with the CD8α subunit, forming a CD8$\alpha\beta$ heterodimer (6, 8). Moreover, CD8 genes are selectively expressed. Although CD8$\alpha\beta$ heterodimers are predominantly found on the surface of TCR$\alpha\beta$ T cells and thymocytes, CD8$\alpha\alpha$ homodimers are additionally expressed on a subset of $\gamma\delta$ T cells, intestinal intraepithelial lymphocytes and natural killer cells (9, 10). Hence, it is safe to conclude that the two sets of CD8 co-receptors subserve distinct functions.

The importance of CD8α in p56^{lck}-linked T cell activation and signaling has been defined by multiple studies (11, 12). Although unable to bind p56^{lck} directly, other findings emphasize the contribution of CD8β to the efficacy of T cell recognition and its ability to broaden the range of antigen recognition (13, 14). Several lines of evidence including our own show that CD8$\alpha\beta$ is a more effective co-receptor than CD8$\alpha\alpha$ in enhancing the sensitivity to peptide antigens as well as alloantigens recognized by TCRs (15, 16). A role for the cytoplasmic portion of the CD8β chain in enhancing Lck kinase activity and promoting T cell development has been suggested (17, 18). In addition, at least for certain TCRs, the contribution of CD8$\alpha\beta$ as a co-receptor may be due, in large part, to its extracellular components (16).

Monoclonal antibody blocking studies, cellular adhesion assays, and direct molecular interaction studies as well as the recent studies of the crystal structures of the Ig domain of the human CD8$\alpha\alpha$ (hCD8$\alpha\alpha$) dimer in complex with HLA-A2 and murine CD8$\alpha\alpha$ (mCD8$\alpha\alpha$) in complex with H-2K^b have shown that the natural ligand of CD8α is the MHC class I molecule (19, 20). These structures show unequivocally that one CD8$\alpha\alpha$ dimer binds to one pMHC complex. Moreover, these findings are consistent with mutational analyses indicating that the α3 loop of the MHC class I (MHCI) molecule is the major CD8α binding component. Although the CD8$\alpha\beta$ heterodimer is thought to bind to the MHCI α3 region as well, currently little is known about the specific molecular details.

Given the importance of understanding the molecular interactions between the CD8 and MHC molecules, recombinant CD8 ectodomain fragments have been produced in a variety of systems (21–28) but without successful secretion of homogeneous products. To overcome this limitation, we expressed the Ig-like domain of mCD8$\alpha\alpha$ or the larger ectodomain fragment utilizing an engineered leucine zipper (LZ) system (29), which we previously applied to the expression of heterodimeric solu-

* This work was supported by National Institutes of Health Grants AI39098 (to H.-C. C.) and AI19807 (to E. L. R.). The costs of publication of this article were defrayed in part by the payment of page charges. This article must therefore be hereby marked "*advertisement*" in accordance with 18 U.S.C. Section 1734 solely to indicate this fact.

‡ Supported by fellowships from the Schweizerische Krebsliga and the Schweizerischer Nationalfond.

§ To whom correspondence should be addressed: Dana-Farber Cancer Inst., 44 Binney St., Boston, MA 02115. Tel.: 617-632-4497; Fax: 617-632-3351; E-mail: hsiu-ching_chang@ dfci.harvard.edu.

[1] The abbreviations used are: TCR, T cell receptor; aa, amino acid(s); MHC, major histocompatibility complex; MHCI, MHC class I; LZ, leucine zipper; ELISA, enzyme-linked immunosorbent assay; mAb, monoclonal antibody; CHO, Chinese hamster ovary; PBS, phosphate-buffered saline; RU, resonance unit(s); CTL, cytotoxic T lymphocyte; PAGE, polyacrylamide gel electrophoresis; wt, wild type.

ble TCR α and β chains. The CD8α Ig-like domain protein purified from Lec3.2.8.1 cells could be readily crystallized (20) in complex with the murine MHC class I H-2K^b molecule loaded with VSV8 octapeptide (30). The same strategy was used to produce the Ig-like domain of soluble recombinant murine CD8$\alpha\beta$ protein as well as the entire extracellular segment. The binding of proteins to pMHC was examined by surface plasmon resonance as well as by functional inhibition studies of killing activity using N15 TCR (29) transgenic (tg) cytolytic T cells. As detailed below, we offer an explanation for the paradox as to why the transmembrane CD8$\alpha\alpha$ *versus* CD8$\alpha\beta$ co-receptors have such large differences in efficiency of facilitating TCR recognition (15, 16) and yet bind to class I MHC with comparable affinities.

EXPERIMENTAL PROCEDURES

Molecular Design and Engineering of Secreted CD8 Co-receptors Using a Heterodimeric Coiled Coil Sequence—To promote the secretion of recombinant dimeric proteins in eukaryotic cells, the N-terminal extracellular segment of the mCD8α chain (residues 1–122) corresponding to the predicted Ig-like domain was fused via a flexible linker (aa residues 123–137) and a thrombin cleavage site (aa residues 129–132) to either Acid-p1 or Base-p1 leucine zipper fragments (31) forming CD8α-A and CD8α-B, respectively (Fig. 1*A*). For this purpose, a 5′-primer encoding aa 1–5 of CD8α and a 3′-primer encoding aa 115–122 plus 10 amino acids of flexible linker were used for polymerase chain reaction of the CD8α Ig-like domain from the pHbAPr-1 neo/Lyt2 cDNA clone (3). The resulting DNA fragment was cloned into the pCR2 vector and sequenced. Subsequently, the error-free CD8α-Ig-like DNA fragment was then digested with *Spe*I and *Bam*HI and ligated with a *Bam*HI-*Spe*I DNA fragment encoding Acid-p1 or Base-p1 peptides to form the CD8α-A and CD8α-B, respectively. The DNA fragments were then subcloned into the *Xba*I site of the pEE14 vector (CellTech Ltd, Berkshire, UK) to form plasmids, pEE14 CD8α-A, and pEE14 CD8α-B, respectively. The CD8β construct pEE14 CD8β-A was generated in a similar fashion using a 5′-primer encoding residues 1–6 of murine CD8β, a 3′-primer encoding CD8β aa 109–115 and 10 amino acids of flexible linker and the CD8β Ig-like domain from pHbAPr-1 neo/Lyt3 cDNA clone (8) as a template. The error-free CD8β Ig-like DNA fragment then was digested with *Xba*I and *Bam*HI and ligated with the *Bam*HI-*Eco*RI DNA fragment encoding Acid-p1 to form the CD8β-A. Subsequently, the DNA fragment was subcloned into the *Xba*I and *Eco*RI site of pEE14 vector to form plasmid, pEE14 CD8β-A. After sequence verification, the pEE14 CD8α-A plus pEE14 CD8α-B cDNAs or pEE14 CD8α-B plus pEE14 CD8β-A cDNAs were pairwise co-transfected into Lec3.2.8.1 cells (32) to produce murine CD8$\alpha\alpha$-LZ or CD8$\alpha\beta$-LZ proteins.

To avoid cysteine mispairing and incorrect disulfide bond formation, a construct encoding the soluble full-length extracellular domain of CD8$\alpha\alpha$ was terminated prior to cysteine residue 166. Moreover, cysteine 151 in the stalk region was mutated to a serine residue. A 5′ oligonucleotide primer corresponded to aa 1–5 of CD8α and a 3′-primer encoding aa 148–165 and 10 amino acids of flexible linker were used to polymerase chain reaction the CD8α_f from the pHbAPr-1 neo/Lyt2 cDNA clone template. The DNA fragments generated were cloned into the pCR2 vector, and sequenced. The error-free CD8α_f DNA fragment then was digested with *Spe*I and *Bam*HI and ligated to the *Bam*HI-*Spe*I DNA fragment encoding Acid-p1 or Base-p1 segments to form CD8α_f-A and CD8α_f-B, respectively. The DNA fragments were then subcloned into the *Xba*I site of pEE14 vector to generate the pEE14 CD8α_f-A and pEE14 CD8α_f-B plasmids. The construction of pEE14 CD8β_f-A was generated in a similar fashion to pEE14 CD8α_f-A, terminating immediately prior to cysteine 150. As with CD8α, the cysteine at aa 137 in the murine CD8β stalk region was mutated to serine. The DNA fragment of the CD8β full-length extracellular domain was generated by polymerase chain reaction from the pHbAPr-1 neo/Lyt3 cDNA clone as a template using the 5′-primer encoding aa 1–6 of CD8β and the 3′-primer encoding aa 135–149 as well as 10 aa of flexible linker. The error-free CD8β_f-A DNA fragment then was digested with *Xba*I and *Bam*HI and ligated to the *Bam*HI-*Eco*RI DNA fragment encoding the Acid-p1 to form the CD8β_f-A. Subsequently, the DNAs were subcloned into the *Xba*I and *Eco*RI sites of pEE14 vector to form the plasmid pEE14 CD8β_f-A. After sequence verification, the pEE14 CD8α_f-A plus pEE14 CD8α_f-B cDNAs or pEE14 CD8α_f-B plus pEE14 CD8β_f-A cDNAs were pairwise co-transfected into Lec3.2.8.1 cells to produce soluble murine CD8$\alpha\alpha_f$-LZ or CD8$\alpha\beta_f$-LZ protein.

Expression of CD8 Ectodomain Fragments Using a Glutamine Synthetase Vector—To produce large quantities of soluble recombinant murine CD8$\alpha\alpha$-LZ protein in Lec3.2.8.1 cells, a method similar to that described in detail for soluble recombinant TCRs (33) was employed. 20 μg of *Sal*I linearized plasmid DNA pEE14 CD8α-A and pEE14 CD8α-B were used for transfection by a calcium phosphate precipitation method using a Transfection MBS kit (Stratagene) following the manufacturer's protocol. 48 h after transfection, the cells were trypsinized, resuspended into 10 ml of Glasgow minimal essential medium-supplemented containing 25 μM methionine sulfoximine and cultured onto 96-well plates. Three to four weeks later, the growing clones were assayed for secretion of soluble CD8$\alpha\alpha$ homodimer by ELISA. In brief, 10 μg/ml of the anti-leucine zipper antibody, 2H11, was coated onto Immulon plate (Dynatech) at room temperature for 2 h, and then the plates were blocked with 1% bovine serum albumin in borate-buffered saline at room temperature for 2 h. 50-μl culture supernatants of individual clone were plated overnight at 4 °C, mixed with 5 μg/ml of biotinylated anti-CD8α mAb 53.6.72 (34) for 2 h, and developed with horseradish peroxidase-conjugated streptavidin (Sigma). The positive clones were picked and transferred to 24-well plates. Subsequently, the highest secretors were ranked by rescreening the supernatants using an indirect capture with the anti-velcro mAb 2H11 (29) on BIAcore (Pharmacia Biosensor) (33). The identical ELISA was used for detection of CD8$\alpha\alpha_f$-LZ proteins. The productions of murine CD8$\alpha\beta$-LZ and CD8$\alpha\beta_f$-LZ were generated similarly using two pairs of *Sal*I linearized plasmid DNAs, pEE14 CD8β-A/pEE14 CD8α-B and pEE14 CD8β_f-A/pEE14 CD8α_f-B, respectively, for transfection into Lec 3.2.8.1 cells. The stable clones producing CD8$\alpha\beta$-LZ or CD8$\alpha\beta_f$-LZ were identified by the ELISA method described above except using 5 μg/ml of biotinylated anti-CD8β mAb YTS156 (35) as the detecting antibody. Transfections of pEE14 CD8α_f-A/pEE14 CD8α_f-B and pEE14 CD8α_f-A/pEE14 CD8β_f-B were performed in CHO cells as well.

Large Scale Production and Purification of CD8 Protein—The transfected Lec3.2.8.1 cell lines producing recombinant soluble CD8 (clones CD8-22-1 for CD8$\alpha\alpha$-LZ, CD8-21-7 for CD8$\alpha\alpha_f$-LZ, CD8-213-16 for CD8$\alpha\beta$-LZ, and CD8-223-34 for CD8$\alpha\beta_f$-LZ) and CHO cells producing recombinant soluble CD8 (clone 15 for CD8$\alpha\alpha_f$-LZ and clone 21 for CD8$\alpha\beta_f$-LZ) were cultured in glutamine-free Glasgow minimal essential medium-supplemented containing 10% dialyzed fetal calf serum and 25 μM methionine sulfoximine and expanded for large scale protein production as described previously (33). The Lec3.2.8.1 supernatants containing the CD8$\alpha\alpha$-LZ fusion proteins were filtered (Corning, 0.22 μM) and immunoaffinity purified using the anti-leucine zipper mAb 2H11 according to an earlier protocol (33). The bound CD8$\alpha\alpha$-LZ was eluted with low pH buffer (20 mM Tris, 50 mM citrate, 0.5 M NaCl, 10% glycerol, pH 4.0, adjusted with NH_4OH) and immediately adjusted to pH 7.0, using 1 M Tris-HCl, pH 9.5. CD8$\alpha\beta$-LZ, CD8$\alpha\alpha_f$-LZ, CD8$\alpha\beta_f$-LZ, CHO-CD8$\alpha\alpha_f$-LZ, and CHO-CD8$\alpha\beta_f$-LZ were purified following a similar procedure. CD8 proteins that were used for cytotoxicity experiments were affinity purified, concentrated to 35–100 mg/ml using a Centricon-10 concentrator (Amicon), and buffer exchanged into PBS, pH 7.2. CD8 proteins that were employed for BIAcore studies were concentrated, sized on a 1.6 × 60 cm Superdex 75 gel filtration column (Amersham Pharmacia Biotech) to remove any aggregates, and then concentrated and equilibrated in PBS. No CD8 aggregates were detected on reanalysis of the gel filtration-sized proteins. The protein concentration of CD8 samples was determined using a Bicinchoninic acid protein assay (Pierce) with bovine serum albumin standards.

BIAcore Studies—All binding studies were performed with PBS/Tween 20 (0.005%) on a BIA1000 surface plasmon resonance biosensor (BIAcore Inc.). To study the CD8-H-2K^b interaction, we took advantage of the CD8 leucine zipper constructs by capturing the CD8-leucine zipper molecules with an anti-leucine zipper mAb coupled to the sensor chip by standard *N*-hydroxysuccinimide/*N*-ethyl-(dimethylaminopropyl) carbodiimide chemistry following standard procedures (BIAcore). This approach aligns all CD8 molecules in a similarly ordered manner, making them accessible for the H-2K^b interaction. Because 2H11 has a relatively fast dissociation rate, we employed an additional mAb, termed 13A12, generated in our laboratory (data not shown). 20 μl of 13A12 at 100 μg/ml in 10 mM NaAc, pH 4.5, were immobilized on a CM5 sensor chip at a flow rate of 5 μl/min resulting in ~5000 RU coupled. CD8$\alpha\alpha_f$-LZ and H-2K^b samples were buffer exchanged into PBS, which is equivalent to the buffer in the reservoir. 20 μl of CD8$\alpha\alpha_f$-LZ (1 μM) were injected onto the 13A12 surface at a flow rate of 10 μl/min. After a 5-min dissociation period, 5 μl/min of H-2K^b-VSV8 (64 μM) were injected onto the 13A12-CD8$\alpha\alpha_f$-LZ surface. This procedure was repeated using H-2K^b-VSV8 concentrations of 1–32 μM. The specificity of

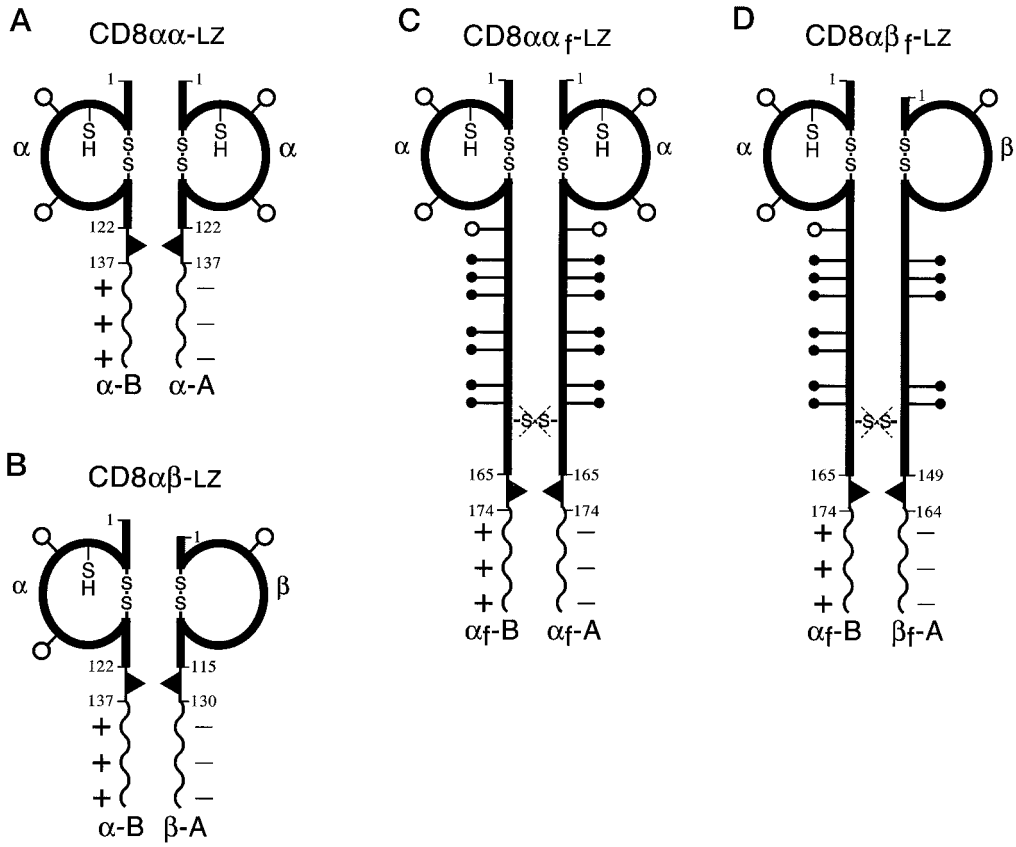

FIG. 1. **Constructs of soluble recombinant murine CD8*αα*-LZ, CD8*αβ*-LZ, CD8*αα*$_f$-LZ, and CD8*αβ*$_f$-LZ.** *A*, schematic representation of mCD8*αα*-LZ showing the Ig-like domain of CD8*α* joined to either an Acid-p1 or a Base-p1 peptide via a flexible linker containing a thrombin cleavage site (indicated by *filled triangle*) to form a dimer of CD8*α*-A and CD8*α*-B, respectively. *B*, CD8*αβ*-LZ consists of the Ig-like domain of CD8*β* joined to Acid-p1 and the CD8*α* joined to Base-p1 forming a dimer of CD8*β*-A and CD8*α*-B. *C*, CD8*αα*$_f$-LZ, the full-length extracellular domain of CD8*α* joined to either an Acid-p1 or a Base-p1 peptide via a flexible linker containing a thrombin cleavage sequence to form a dimer of CD8*α*$_f$-A and CD8*α*$_f$-B, respectively. *D*, CD8*αβ*$_f$-LZ, the full-length extracellular domain of CD8*β* joined to Acid-p1 to form CD8*β*$_f$-A in noncovalent association with CD8*α*$_f$-B. The positions of cysteines that were mutated to serines to exclude disulfide bond formation are marked with *crossed dotted lines*. The potential *N*-linked glycosylation sites (at CD8*α* aa 43, 70 and 123 and at CD8*β* aa 13) and *O*-linked glycosylation sites (at CD8*α* aa 124–127, 133, 135, 140, 142, and 143 and at CD8*β* aa 120, 121, 124, 127, and 128) are schematically represented by *open* and *filled lollipops*, respectively. The unpaired cysteine (aa 37) in CD8*α* is denoted (*SH*).

the binding was assured by H-2K^b injections (1–64 μM) directly onto the 13A12 surface (data not shown). The specific RU for H-2K^b-CD8*αα*$_f$-LZ binding at equilibrium were determined by subtracting background RU (H-2K^b on the 13A12 surface) from the total RU. The K_d was derived from a Scatchard plot RU/concentration *versus* RU and linear regression analysis (Kaleidagraph software). The experiment was repeated three times with CD8*αα*-LZ and CD8*αα*$_f$-LZ, and only once with CD8*αβ*-LZ, CD8*αβ*$_f$-LZ, CHO-CD8*αα*$_f$-LZ, and CHO-CD8*αβ*$_f$-LZ. For all BIAcore studies, the H-2K^b *α*-chain (residues 1–274) and the murine-*β*2-microglobulin (residues 1–99) were expressed as separate inclusion bodies in *Escherichia coli* and refolded in the presence of VSV8 peptide as described earlier (30).

Cytotoxicity Assays—To obtain N15 CTL, splenocytes were isolated from Rag2$^{-/-}$ mice expressing a transgenic N15 TCR (36) and stimulated to obtain a short term cytotoxic T cell line as described previously (37). For stimulation, the splenocytes were co-cultured in 24-well plates (5×10^6 cells/well) with irradiated N1 cells (5×10^5 cells/well). N1 cells constitutively present the cognate VSV8 peptide as an expressed minigene. After 5–7 days of culture with rat-derived concanavalin A supernatants, N15TCR$^+$ CTLs were harvested and used as effector cells in the cytotoxicity assay. 1×10^6 EL-4 target cells were labeled with 80 μCi of sodium [^{51}Cr]chromate for 1 h at 37 °C. After four washings with RPMI complete, the K^b-expressing EL-4 cells were resuspended at 50,000 cells/ml in complete RPMI and transferred into 96-well U bottom plates (100 μl/well). To determine a suboptimal dose of peptide for inhibitory experiments, peptides were added at concentrations between 10^{-6} and 10^{-12} M in a final volume of 100 μl of complete RPMI and incubated for 1 h. Finally, CTLs (100 μl) were added at an E:T ratio of 10:1 or 5:1, and ^{51}Cr release was determined using standard conditions (36). In the actual blocking experiment, EL-4 cells were pulsed with VSV8 at 2×10^{-10} M. As a negative control either SEV9 (irrelevant peptide) or only PBS was added to the wells. Anti-CD8*α* 53.6.72 mAb was used as positive control, whereas a two-domain recombinant CD4 (rCD4) (38) was used as a negative control for blocking experiments. 1 μM 53.6.72 mAb was added to CTL cells for 10 min at room temperature. CD8*αα*-LZ, CD8*αβ*-LZ, CD8*αα*$_f$-LZ, CD8*αβ*$_f$-LZ, CHO-CD8*αα*$_f$-LZ, and CHO-CD8*αβ*$_f$-LZ were concentrated using a Centricon-10 (Amicon), and 27.5–220 μM (final concentration) of CD8 protein or 27.5–220 μM of rCD4 were added to the antigen presenting cells 10 min prior to addition of 5×10^4 N15 CTL (in 100 μl)/well. To determine background release, 100 μl of RPMI completed medium was added to ^{51}Cr-labeled targets. The maximal ^{51}Cr release was quantitated by adding 100 μl of 1% Triton X to ^{51}Cr-labeled target cells. After 4 h at 37 °C, the plates were centrifuged, and 50% of the well solution was removed and counted in a γ-counter.

RESULTS

Design of Secreted Dimeric CD8αα and CD8αβ Ig-like Ectodomains Using a Leucine Zipper Sequence and Expression in Lec3.2.8.1 Cells—A strategy to promote secretion of various soluble recombinant CD8 co-receptor protein fragments with homogeneous glycan adducts in the Lec3.2.8.1 eukaryotic cells was developed. To this end, a set of CD8 co-receptor constructs was produced as depicted schematically in Fig. 1. For example, the N-terminal extracellular segment of the mCD8*α* chain (residues 1–122) corresponding to the predicted Ig-like domain was fused via a flexible linker (residues 123–137) and a thrombin cleavage site to either an Acid-p1 or Base-p1 30-aa-long leucine zipper fragment to form CD8*α*-Acid (CD8*α*-A) and CD8*α*-Base (CD8*α*-B), respectively (Fig. 1*A*). Subsequently, cDNAs encod-

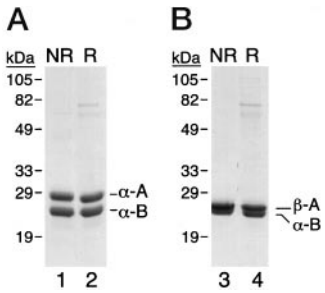

FIG. 2. **SDS-PAGE analysis of recombinant CD8 proteins.** *A*, Coomassie staining of affinity purified CD8αα-LZ protein run on 12.5% SDS-PAGE gel under nonreducing (*NR*, *lane 1*) and reducing conditions (*R*, *lane 2*). The positions of CD8α-A and CD8α-B monomers are indicated. *B*, Coomassie staining of affinity purified mCD8αβ-LZ protein run on 12.5% SDS-PAGE gel under nonreducing (*NR*, *lane 3*) and reducing (*R*, *lane 4*) conditions. The positions of CD8β-A and CD8α-B monomers were determined by N-terminal amino acid sequencing as indicated.

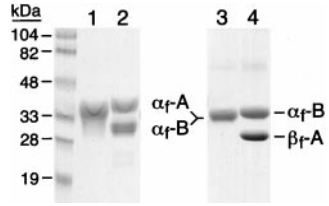

FIG. 3. **SDS-PAGE analysis of CD8αα$_f$-LZ and CD8αβ$_f$-LZ proteins produced in CHO and Lec3.2.8.1 cells.** Coomassie-stained gel of affinity purified CHO-produced CD8αα$_f$-LZ and CD8αβ$_f$-LZ protein (*lanes 1* and *2*, respectively) and corresponding Lec3.2.8.1-produced CD8αα$_f$-LZ (*lane 3*) and CD8αβ$_f$-LZ (*lane 4*) after resolution by 12.5% SDS-PAGE under nonreducing conditions. The positions of CD8α$_f$-A, CD8α$_f$-B, and CD8β$_f$-A subunits are indicated for the Lec3.2.8.1-produced material.

ing CD8α-A and CD8α-B were transfected into Lec3.2.8.1 cells, and clones secreting the CD8αα ectodomain were screened by ELISA. mCD8αα-LZ protein was then affinity purified from the producer clone CD8-22-1 using the anti-leucine zipper mAb 2H11. As shown in Fig. 2*A*, under either nonreducing conditions (*NR*, *lane 1*) or reducing conditions (*R*, *lane 2*), the recombinant mCD8αα-LZ protein runs in the Coomassie-stained SDS-PAGE gel as two bands corresponding to CD8α-A and CD8α-B monomer components with apparent molecular masses of 29 and 25 kDa, respectively. The difference in mobility of the CD8α chains is a consequence of the divergent charges within the appended acid or basic leucine zipper sequences. By this analysis, the affinity purified mCD8αα-LZ material is ~90% pure with a 1:1 ratio of CD8α-A and CD8α-B. Although not shown, gel filtration chromatography on Sephadex 75 demonstrated that mCD8αα-LZ was dimeric and readily removed the trace amount of higher molecular mass contaminants and/or aggregates. Moreover, the expected N-terminal sequence of mCD8αα-LZ was verified by amino acid sequencing (not shown).

The same strategy was then applied to the expression of the CD8αβ Ig-like domains in Lec 3.2.8.1. cells. The N-terminal extracellular segment of the mCD8β chain (residues 1–115) corresponding to the predicted Ig-like domain was fused via a flexible linker (residues 116–130) containing a thrombin cleavage site to the Acid-p1 peptide to yield CD8β-Acid (CD8β-A) (Fig. 1*B*). The cDNA encoding the CD8β-A subunit was engineered into the pEE14 vector. Subsequently, the pEE14 CD8α-B and pEE14 CD8β-A plasmids were co-expressed in Lec3.2.8.1 cells, CD8αβ producing clones were identified by ELISA and mCD8αβ-LZ protein immunoaffinity purified using the anti-leucine zipper mAb 2H11. As shown in Fig. 2*B*, under nonreducing conditions (*NR*, *lane 3*) and reducing conditions (*R*, *lane 4*), the recombinant mCD8αβ-LZ runs as closely spaced CD8β-A and CD8α-B monomers at molecular masses 26 and 25 kDa, respectively. Because the α- and β- bands in the CD8αβ-LZ SDS-PAGE could not be separated, CD8αβ-LZ was first digested with endoglycosidase-H (0.02 unit/mg CD8αβ-LZ for 2 h at 37 °C) and then resolved by SDS-PAGE. Following deglycosylation, the CD8α-B derivative runs at 20 kDa and the CD8β-A derivative runs at 24 kDa. This differential mobility permitted N-terminal sequencing of the subunits that confirmed the identity of the individual chains and suggested a 1:1 ratio of CD8α-B and CD8β-A (data not shown). As shown in Fig. 2*B*, the immunoaffinity purified mCD8αβ-LZ material is ~90% pure. The 2H11 mAb-purified mCD8αβ-LZ protein expresses the native epitopes recognized by five distinct anti-CD8α mAbs (53.6.72, 19/178, H59–101.7, YTS105, and YTS169) (34, 35, 39) and four anti-CD8β mAbs (53.5.8, H35–17, YTS156.7, and KT112) (34, 35, 39, 40), as measured by BIAcore binding studies (data not shown).

Expression of the Full-length sCD8αα and sCD8αβ Ectodomains—The stalk region that connects the CD8α and CD8β Ig domain to the cell membrane contains ~44 aa residues in the α chain and ~35 aa residues in the β chain (depending on species). To assess the functional contribution of *O*-linked glycans in the stalk region of CD8 to MHC class I binding, we expressed the soluble full-length sCD8αα$_f$ and sCD8αβ$_f$ in wt CHO cells or the glycosylation mutant Lec3.2.8.1. The former expression system synthesizes proteins with full-length glycan adducts. In contrast, Lec3.2.8.1 cells produce glycoproteins with all *N*-linked carbohydrates truncated to the Man_5 form and *O*-linked carbohydrate truncated to a single GalNAc (32).

Several reports indicated that the formation of disulfide-linked homodimers is extremely inefficient when the entire native ectodomain of either hCD8αα or rat CD8αα was expressed. The resulting products contained a mixture of disulfide- and nondisulfide-linked CD8 homodimers, monomers, and aggregates (21–24, 26, 41). To avoid this complexity, the extracellular segment of the mCD8α chain (residues 1–165) N-terminal to the last extracellular cysteine was fused to either an Acid-p1 or Base-p1 to form CD8α$_f$-A and CD8α$_f$-B, respectively (Fig. 1*C*). Furthermore, the cysteine residue at aa 151 of CD8α was converted to serine by polymerase chain reaction mutagenesis to obviate disulfide scrambling. Both cDNAs were engineered into the pEE14 vector system and expressed in CHO or Lec3.2.8.1 cells. To express the full-length mCD8αβ$_f$-LZ, the CD8β cysteine at position 137 was similarly mutated to serine, and the extracellular segment of the mCD8β chain (residues 1–149) was fused to an Acid-p1 forming CD8β$_f$-A. The pEE14 CD8α$_f$-B and pEE14 CD8β$_f$-A plasmids were co-transfected to generate stable cell lines, producing mCD8αβ$_f$-LZ as described under "Experimental Procedures." Lec3.2.8.1 or wt CHO secreted mCD8αα$_f$-LZ and mCD8αβ$_f$-LZ were affinity purified from culture supernatants using the 2H11 mAb.

As shown in Fig. 3, under nonreducing conditions, the wt CHO-produced recombinant mCD8αα$_f$-LZ runs as one broad band of apparent molecular mass of 30–37 kDa (Fig. 3, *lane 1*). By contrast, the Lec3.2.8.1-produced recombinant mCD8αα$_f$-LZ protein runs as a discrete band with a molecular mass of 32 kDa (lane 3). The wt CHO-produced recombinant mCD8αβ$_f$-LZ runs as two rather broader bands representing CD8α$_f$-B and CD8β$_f$-A subunits at molecular masses 35 and 30 kDa, respectively (Fig. 3, *lane 2*), whereas Lec3.2.8.1-produced recombinant mCD8αβ$_f$-LZ runs as discrete bands of molecular masses 32 and 29 kDa (*lane 4*). The difference in the molecular masses of these products reflects the different nature of the glycosylated adducts. The affinity purified mCD8αβ$_f$-LZ material is quite pure and shows a 1:1 ratio of CD8α$_f$-B and CD8β$_f$-A in Coomassie gel (Fig. 3). The affinity puri-

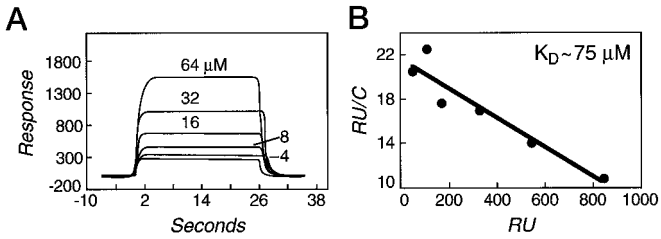

FIG. 4. **Affinity measurement of the CD8αα class I MHC interaction.** Shown are the BIAcore sensorgrams of H-2K^b/VSV8 binding to chip-bound CD8αα$_f$-LZ captured by mAb 13A12 (*A*) and corresponding Scatchard analysis of H-2K^b/VSV8 binding to CD8αα$_f$-LZ (*B*).

fied mCD8 molecules bear native epitopes as measured by BIAcore analysis using multiple mAbs reactive with CD8 co-receptors found on T lymphocytes (see below).

BIAcore Affinity Measurements—The interactions between soluble CD8 and MHC class I H-2K^b (complexed to VSV8) were examined using an SPR biosensor, which allows direct measurement of kinetic interactions between immobilized and solution-phase molecules (42). The affinity for H-2K^b-VSV8 was measured using all six different CD8 protein derivatives (CD8αα-LZ, CD8αβ-LZ, CD8αα$_f$-LZ, CD8αβ$_f$-LZ, CHO-CD8αα$_f$-LZ, and CHO-CD8αβ$_f$-LZ). The proper folding of these soluble CD8 proteins was confirmed by BIAcore analysis using anti-CD8α (YTS169, 19/178, 53.672, H59–101.7, YTS105) and anti-CD8β mAbs (YTS156.7, H35-17, 53.5.8, KT112) for binding studies of the CD8 proteins captured on the 13A12 anti-leucine zipper mAb surface (data not shown). For affinity measurements, 20 μl of the individual CD8αα or CD8αβ (at 1 μM) proteins were first captured by 13A12 on the chip. Subsequently, VSV8/K^b was injected at 1–64 μM concentrations. Fig. 4 shows a typical sensorgram of the H-2K^b binding to CD8αα$_f$-LZ. As a control, H-2K^b at identical concentrations of 1–64 μM was injected on a 13A12 mAb surface alone. Although not shown, only residual nonspecific binding was detected. Because the association and dissociation phases were too fast to analyze, the equilibrium binding constant was determined using Scatchard analysis. Independent experiments have been carried out three times for both CD8αα-LZ and CD8αα$_f$-LZ, and only once for CD8αβ-LZ, CD8αβ$_f$-LZ, CHO-CD8αα$_f$-LZ, and CHO-CD8αβ$_f$-LZ. For Scatchard plots, VSV8/K^b concentrations of 4–64 μM or 8–64 μM have been used. Table I summarizes the affinities of the different CD8 proteins for pMHCI. As shown, CD8αα$_f$-LZ has an affinity of 35–75 μM for H-2K^b-VSV8, whereas that of CD8αβ$_f$-LZ is comparable at 67 μM. Moreover, CD8 constructs lacking the C-terminal stalk regions (CD8αα-LZ and CD8αβ-LZ) have comparable affinity to the full-length CD8αα$_f$ and CD8αβ$_f$, implying that the Ig domain is necessary and sufficient for MHC binding. Moreover, CD8αα-LZ and CD8αβ-LZ affinities of 57–86 and 30 μM, respectively, are quite similar.

CD8 on the T cell surface is known to be heavily *O*-linked glycosylated in the stalk region and to possess a sialylated Ig domain. Thus, it was of interest to investigate whether the fully glycosylated CHO-produced full-length CD8 proteins differ in their affinities for pMHC relative to Lec3.2.8.1-derived proteins. However, CHO-CD8αα$_f$-LZ showed an affinity of 64 μM, and CHO-CD8αβ$_f$-LZ showed an affinity of 22 μM. Based on these results in comparison to the Lec 3.2.8.1. derivatives, there appears to be no difference in affinity (within a factor of <3) for K^b resulting from the distinct glycosylation pattern of the CD8 protein.

sCD8αα and sCD8αβ Are Able to Block the Cytotoxic Activity of N15 CTL—Next we tested the ability of sCD8 molecules to functionally inhibit the cytolytic activity of class I MHC-dependent N15 CTL derived from N15 tg Rag2$^{-/-}$ H-2^b mice. In these experiments, CTLs were added at an E:T ratio of 5:1 to ^{51}Cr-labeled EL-4 cells pulsed with 2×10^{-10} M VSV8 peptide, and ^{51}Cr release was determined in the presence or absence of CHO-CD8αα$_f$-LZ or CHO-CD8αβ$_f$-LZ proteins. Anti-CD8α 53.6.72 (1 μM) was used as positive control, and a two-domain recombinant CD4 (rCD4) (38) was used as a negative control for the blocking experiments. Fig. 5*A* shows the results of one representative experiment when the CD8 ectodomain dimers were added to EL-4 cells for 10 min prior to the cytotoxicity assay. Both CHO-CD8αα$_f$-LZ and CHO-CD8αβ$_f$-LZ proteins are able to block the cytotoxic activity of N15 CTL in a dose-dependent fashion, inhibiting 81.1 and 73.7%, respectively, at a 220 μM concentration. The concentration of soluble CD8 necessary for 50% functional inhibition (55–110 μM) correlates with the affinities of the CD8 dimers for class I MHC as measured by BIAcore. At 110 μM soluble CHO-CD8αβ$_f$-LZ inhibited slightly better than CHO-CD8αα$_f$-LZ at the same molar concentration. Note that anti-CD8α antibody 53.6.72 inhibited killing by about 95%, whereas rCD4 showed a negligible percentage of inhibition.

To address whether the Ig-like domains of the CD8 dimer alone were able to mediate functional CTL inhibition, we compared the effects of CD8αα-LZ and CD8αβ-LZ with those of CHO-CD8αα$_f$-LZ and CHO-CD8αβ$_f$-LZ. Fig. 5*B* shows results for all four CD8 ectodomain dimer fragments at 220 μM. The CD8 Ig-like domain *per se*, in absence of the stalk region and complex glycans, is able to block cytolytic function. Compared with the CHO derivatives, Lec 3.2.8.1 CD8αα-LZ only inhibited 36.5%, whereas Lec 3.2.8.1 CD8αβ-LZ inhibited 48.5%. Thus, the level of CTL inhibition with CD8αα-LZ and CD8αβ-LZ is somewhat lower than that observed with the CHO-produced full-length ectodomain CD8αα$_f$-LZ and CD8αβ$_f$-LZ protein. Whether the CD8 stalk region in the CD8αα$_f$-LZ and CD8αβ$_f$-LZ derivatives contributes to the functional inhibition by affecting additional components of the CTL or target cell surface is unknown. It is also possible that the greater size of the CHO-CD8αα$_f$-LZ and CHO-CD8αβ$_f$-LZ protein relative to the Lec3.2.8.1 CD8αα-LZ and CD8αβ-LZ proteins creates an additional steric inhibition that facilitates the observed functional blockade.

TABLE I
Affinities of CD8 constructs for H-2K^b-VSV8 as measured by surface plasmon resonance

Soluble recombinant CD8	CD8 constructs	Cell line expressed	K_d[a]
			μM
CD8αα-LZ	Ig-like domain	Lec3.2.8.1	57, 58, 86
CD8αβ-LZ	Ig-like domain	Lec3.2.8.1	30
CD8αα$_f$-LZ	Full-length extracellular domain	Lec3.2.8.1	35, 74, 75
CD8αβ$_f$-LZ	Full-length extracellular domain	Lec3.2.8.1	67
CHO-CD8αα$_f$-LZ	Full-length extracellular domain	CHO	64
CHO-CD8αβ$_f$-LZ	Full-length extracellular domain	CHO	22

[a] K_d values were determined at 25 °C. Individual values determined from independent experiments using Scatchard analysis are shown.

DISCUSSION

Various CD8 co-receptor ectodomain dimers were produced in soluble form to investigate the basis for differences in the functions of αα and αβ dimers and the contribution of their respective Ig-like domain and stalk region segments. The yield of immunoaffinity purified protein derived from each construct

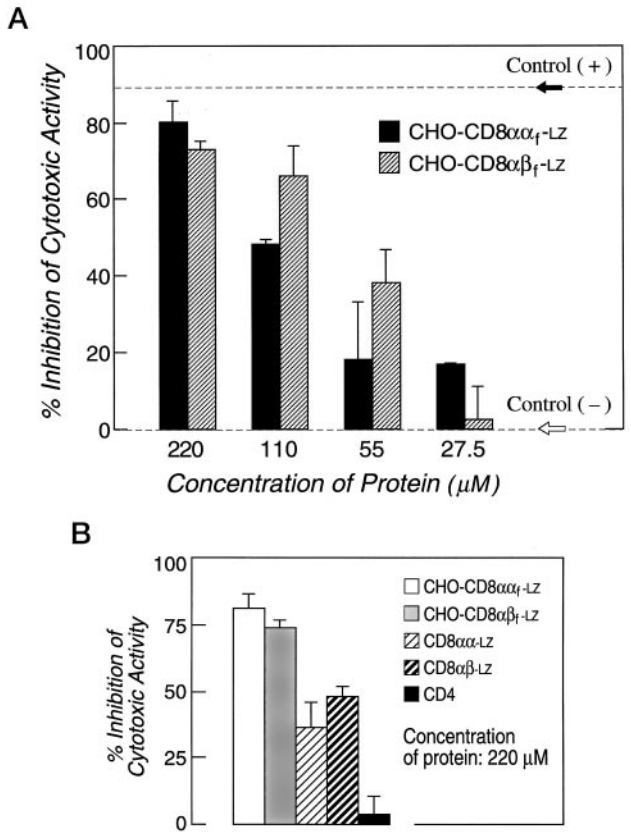

FIG. 5. **Soluble recombinant CD8αα and CD8αβ dimer fragments functionally block the cytotoxic activity of N15tg CTL to equivalent degrees.** *A*, indicated concentrations of wt CHO-produced mCD8αα$_f$-LZ and mCD8αβ$_f$-LZ were added to a cytotoxic assay using N15 CTL effectors generated from splenocytes of N15 TCR transgenic Rag2$^{-/-}$ mice and EL4 cells pulsed with VSV8 peptide (2×10^{-10} M) as target cells at an E:T ratio of 5:1. The ability of anti-CD8α mAb 53.6.72 (positive control) and a two-domain rCD4 (negative control) to inhibit lysis is indicated by the *solid arrow* and *open arrow*, respectively. *B*, 220 μM concentrations of CHO-CD8αα$_f$-LZ, CHO-CD8αβ$_f$-LZ, CD8αα-LZ, and CD8αβ-LZ as well as two-domain recombinant CD4 were added into the above cytotoxicity.

expressed in Lec3.2.8.1 cells was substantial: 12–15 mg/liter for mCD8αα (CD8αα-LZ) or 8–10 mg/liter for mCD8αβ (CD8αβ-LZ). The levels of expression of sCD8 compare favorably with previous reports of the expression of hCD8αα (~2 mg/liter of affinity purified CD8αα) and the *E. coli*-produced Ig-like domain of hCD8αα (~0.5 mg/liter). The well paired CD8αα homodimer expressed in the glycosylation-defective mutant, Lec3.2.8.1, cell system has already provided adequate materials for crystallization of the complex of CD8αα/K^b (20). The high level expression of mCD8αβ should allow a detailed structural analysis of CD8αβ/K^b alone or in complex with a class I MHC-restricted TCR as well.

When the CD8αα dimer containing both cysteine residues in the stalk region was expressed in early studies (22–24, 26, 27, 41), the majority of the recombinant protein was monomeric, caused by intrachain pairing of the two cysteine residues in the stalk region (21). In contrast, the results of SDS-PAGE (Figs. 2 and 3) and gel filtration here indicate that the subunit products of CD8αα$_f$-LZ and CD8αβ$_f$-LZ are in a molar ratio of 1:1 with minor or no aggregates. This result suggests that the mutation to serine of the cysteine residue at aa 151 of CD8α or aa 137 of CD8β in the stalk region avoided the disulfide bond scrambling completely. The yield of immunoaffinity purified full-length ectodomain using the anti-leucine zipper mAb, 2H11, was 8–15 mg/liter for CD8αα$_f$-LZ and CD8αβ$_f$-LZ expressed in CHO or Lec3.2.8.1 cells. Moreover, the affinity purified mCD8 molecules are in a native configuration as measured by BIAcore using five anti-CD8α mAbs and four anti-CD8β antibodies.

The stalk region connecting the Ig-like domain of mCD8 to the membrane consists of ~44 aa in the α chain and ~35 aa in the β chain (Fig. 1*A*). Each connecting peptide must be extended because it is rich in proline residues and contains a number of *O*-linked glycans. The biological function of these stalks is unclear as is the precise orientation of the TCR chains relative to the co-receptor subunits. However, the sialic acid content of CD8β *O*-linked glycans decreases significantly on thymocytes and activated T cells compared with the levels found on resting T cells (43–45), a phenomenon not observed for the CD8α chain. The results imply that the ability of CD8β to vary its overall charge and glycan size may have important consequences for CD8-TCR interaction. To examine the functional contribution of the *O*-linked glycan in the stalk region of CD8, we expressed the soluble full-length sCD8αα and sCD8αβ in wt CHO cells or in the glycosylation mutant Lec3.2.8.1, allowing a direct comparison of the importance of the complex sugars to the MHC binding function of CD8. A cytotoxicity assay utilizing the N15 CTL derived from N15 tg Rag2$^{-/-}$ H-2^b mice then assessed the ability of soluble CD8 molecules to inhibit the cytolytic activity of class I MHC-dependent N15 CTL. The results of two independent experiments show that CHO-produced CD8αα$_f$-LZ and CHO-CD8αβ$_f$-LZ proteins are able to block the cytotoxic activity of N15 CTL in a dose-dependent fashion, with no significant difference between the CHO-CD8αα$_f$-LZ and CHO-CD8αβ$_f$-LZ proteins. This result implies that the binding of soluble CD8αα or CD8αβ to MHC class I molecules on target cells must be equivalent. These results are consistent with the BIAcore analysis showing similar K^b binding for CD8αα and CD8αβ dimers (Table I). Moreover, both the Lec3.2.8.1-produced CD8αα and CD8αβ Ig-like domains, without the stalk region, are able to block cytolytic function.

The affinity of CD8 to H-2K^b-VSV8 has been measured using all six different CD8 constructs produced (Table I). CD8αα$_f$-LZ has an affinity of ~62 μM (n = 4) for H-2K^b-VSV8, and CD8αβ$_f$-LZ show a slightly higher affinity of ~44 μM (n = 2). CD8 constructs lacking the C-terminal stalk regions, CD8αα-LZ and CD8αβ-LZ, do not appear to have lower affinity (~67 μM (n = 3) and 30 μM (n = 1)) than their full-length protein counterparts (Table I). These affinities are comparable with those determined previously by Garcia *et al.* (46). In that report, the full-length ectodomains of mCD8αα and mCD8αβ expressed with a histidine tag in a *Drosophila* system reveal a moderate affinity (~39 and ~11 μM, respectively) to MHC class I molecules loaded with different antigenic peptides, with the CD8αβ heterodimer having a slightly better affinity. However, the results are substantially different from the affinity measured by Wyer *et al.* (28). Utilizing the *E. coli*-expressed recombinant Ig-like domain of hCD8αα, the affinity of hCD8αα to pMHCI was determined to be greater than 200 μM (28). Species differences, allelic differences, the absence of the mucin-like stalk region for sCD8, and/or the presence of aggregated materials might explain these discrepancies. In the present expression system, Lec3.2.8.1-produced CD8 protein shows very little difference from the CHO-produced CD8. These findings imply no substantial difference in affinity because of the glycosylation pattern of the stalk region of the CD8αα or CD8αβ. Furthermore, they show that greater affinity is not the basis by which the CD8αβ heterodimer has a much more significant effect relative to the CD8αα homodimer in influencing TCR/pMHC binding on the T cell surface (14–16, 47–50).

The overall structure of the mCD8αα/VSV8/H-2K^b complex

determined crystallographically reveals a single VSV8/H-2K^b molecule interacting with one mCD8αα homodimer (20). The asymmetric arrangement of the α3 and β_2M domains of the H-2K^b molecule creates a concave shape underneath the H-2K^b α2 domain, suitable for accommodating a mCD8αα dimer. This CD8αα dimer binds in an antibody-like manner to the protruding H-2K^b α3 CD loop, using all six CDR-like loops for the interaction. The binding to H-2K^b is asymmetric; in particular, the N terminus of CD8α1 (the "top" subunit) is buried between the β_2M and the α3 domain of the MHC molecule, in contrast to its counterpart in CD8α2 (the "bottom" subunit), which is exposed to solvent as well as involved in crystal contacts. A similar picture was reported for the human CD8αα interaction with HLA-A2 (19).

Currently, the details of molecular interaction of CD8αβ with MHC class I is unknown. It was proposed by Gao *et al.* (19), based on scoring favorable electrostatic interactions, that the hCD8β subunit of hCD8αβ heterodimer may replace the bottom subunit of the hCD8αα homodimer. Recently, the finding that coexpression of the mutant R4A of hCD8α and wt hCD8β on CD8αβ heterodimers on COS cells failed to facilitate MHC class I molecular binding (25) leads to the conclusion that CD8α, not CD8β, provides the majority of contacts with MHC class I. However, replacing either of the mCD8α subunits in the mCD8αα homodimer structure with a mCD8β model by molecular graphic modeling and visual inspection of these models did not allow us to infer the localization of CD8β. Nevertheless, the mCD8α stalk consists of 29 residues including seven potential *O*-glycosylation sites prior to the first interchain disulfide bond. The corresponding N-terminal motif in the CD8β stalk has only 22 residues, containing two prolines and five potential *O*-glycosylation sites. Given these differences, it is reasonable to suggest that the longer CD8α subunit stalk rather than that of CD8β prefers to extend a greater distance so that CD8α lies in a position analogous to CD8α2, whereas CD8β replaces the top CD8α1 subunit position. In this proposed orientation, the CD8αβ co-receptor would be thermodynamically more efficient. The CD8β stalk is shorter and the CD8α is longer, thus offering a presumably preconfigured co-receptor for interaction with MHC class I. This preconfiguration may be largely responsible for CD8αβ co-receptor efficiency. Experiments aimed at testing this possibility are in progress.

Acknowledgments—We thank Drs. Linda Clayton and Jerome Ritz for critical reading of the manuscript.

REFERENCES

1. Miceli, M. C., and Parnes, J. R. (1993) *Adv. Immunol.* **53,** 59–122
2. Littman, D. R., Thomas, Y., Maddon, P. J., Chess, L., and Axel, R. (1985) *Cell* **40,** 237–246
3. Zamoyska, R., Vollmer, A. C., Sizer, K. C., Liaw, C. W., and Parnes, J. R. (1985) *Cell* **43,** 153–163
4. Nakauchi, H., Nolan, G. P., Hsu, C., Huang, H. S., Kavathas, P., and Herzenberg, L. A. (1985) *Proc. Natl. Acad. Sci. U. S. A.* **82,** 5126–5130
5. Norment, A. M., and Littman, D. R. (1988) *EMBO J.* **7,** 3433–3439
6. DiSanto, J. P., Knowles, R. W., and Flomenberg, N. (1988) *EMBO J.* **7,** 3465–3470
7. Moebius, U., Kober, G., Griscelli, M. L., Hercend, T., and Meuer, S. C. (1991) *Eur. J. Immunol.* **21,** 1793–1800
8. Gorman, S. D., Sun, Y. H., Zamoyska, R., and Parnes, J. R. (1988) *J. Immunol.* **140,** 3646–3653
9. Poussier, P., and Julius, M. (1994) *Annu. Rev. Immunol.* **12,** 521–553
10. von Boehmer, H. (1990) *Annu. Rev. Immunol.* **8,** 531–556
11. Veillette, A., Bookman, M. A., Horak, E. M., and Bolen, J. B. (1988) *Cell* **55,** 301–308
12. Letourneur, F., Gabert, J., Cosson, P., Blanc, D., Davoust, J., and Malissen, B. (1990) *Proc. Natl. Acad. Sci. U. S. A.* **87,** 2339–2343
13. Karaki, S., Tanabe, M., Nakauchi, H., and Takiguchi, M. (1992) *J. Immunol.* **149,** 1613–1618
14. Wheeler, C. J., Hoegen von, P., and Parnes, J. R. (1992) *Nature* **357,** 247–249
15. Renard, V., Romero, P., Vivier, E., Malissen, B., and Luescher, I. F. (1996) *J. Exp. Med.* **184,** 2439–2444
16. Witte, T., Spoerl, R., and Chang, H.-C. (1999) *Cell Immunol.* **191,** 90–96
17. Itano, A., Cado, D., Chan, F. K., and Robey, E. (1994) *Immunity* **1,** 287–290
18. Irie, H. Y., Mong, M. S., Itano, A., Crooks, M. E., Littman, D. R., Burakoff, S. J., and Robey, E. (1998) *J. Immunol.* **161,** 183–191
19. Gao, G. F., Tormo, J., Gerth, U. C., Wyer, J. R., McMichael, A. J., Stuart, D. I., Bell, J. I., Jones, E. Y., and Jakobsen, B. K. (1997) *Nature* **387,** 630–634
20. Kern, P., Teng, M.-K., Smolyar, A., Liu, J.-H., Liu, J., Hussey, R. E., Chang, H.-C., Reinherz, E. L., and Wang, J.-H. (1998) *Immunity* **9,** 519–530
21. Leahy, D. J., Axel, R., and Hendrickson, W. A. (1992) *Cell* **68,** 1145–1162
22. Alcover, A., Herve, F., Boursier, J.-P., Spagnoli, G., Olive, D., Mariuzza, R. A., and Acuto, O. (1992) *Mol. Immunol.* **30,** 55–67
23. Boursier, J.-P., Alcover, A., Herve, F., Laisney, I., and Acuto, O. (1993) *J. Biol. Chem.* **268,** 2013–2020
24. Classon, B. J., Brown, M. H., Garnett, D., Somoza, C., Barclay, A. N., Willis, A. C., and Williams, A. F. (1992) *Int. Immunol.* **4,** 215–225
25. Devine, L., Sun, J., Barr, M. R., and Kavathas, P. B. (1999) *J. Immunol.* **162,** 846–851
26. Meyerson, H. J., Huang, H.-H., Fayen, J. D., H.-M., T., Getty, R. R., Greenspan, N. S., and Tykocinski, M. L. (1996) *J. Immunol.* **156,** 574–584
27. Garcia, K. C., Degano, M., Stanfield, R. L., Brunmark, A., Jackson, M. R., Peterson, P. A., Teyton, L., and Wilson, I. A. (1996) *Science* **274,** 209–219
28. Wyer, J. R., Wilcox, B. E., Gao, G. F., Gerth, U. C., Davis, S. J., Bell, J. P., van der Merwe, P. A., and Jakobsen, B. K. (1999) *Immunity* **10,** 219–225
29. Chang, H.-C., Bao, Z.-Z., Yao, Y., Tse, A. G. D., Goyarts, E. C., Madsen, M., Kawasaki, E., Brauer, P. P., Sacchettini, J. C., Nathenson, S. G., and Reinherz, E. L. (1994) *Proc. Natl. Acad. Sci. U. S. A.* **91,** 11408–11412
30. Zhang, W., Young, A. C. M., Imarai, M., Nathenson, S. G., and Sacchettini, J. C. (1992) *Proc. Natl. Acad. Sci. U. S. A.* **89,** 8403–8407
31. O'Shea, E. K., Lumb, K. J., and Kim, P. S. (1993) *Curr. Biol.* **3,** 658–667
32. Stanley, P. (1989) *Mol. Cell. Biol.* **9,** 377–383
33. Liu, J., Tse, A. G. D., Chang, H.-C., Liu, J., Wang, J., Hussey, R., Chisthi, Y., Reinhold, B., Spoerl, R., Nathenson, S. G., Sacchettini, J. C., and Reinherz, E. L. (1996) *J. Biol. Chem.* **271,** 33639–33646
34. Ledbetter, J., and Herzenberg, L. (1979) *Immunol. Rev.* **47,** 63–90
35. Qin, S., Cobbold, S., Benjamin, R., and Waldmann, H. (1989) *J. Exp. Med.* **169,** 779–794
36. Ghendler, Y., Hussey, R. E., Witte, T., Mizoguchi, E., Clayton, L. K., Bhan, A. K., Koyasu, S., Chang, H.-C., and Reinherz, E. L. (1997) *Eur. J. Immunol.* **27,** 2279–2289
37. Shibata, K.-I., Imarai, M., van Bleek, G. M., Joyce, S., and Nathenson, S. G. (1992) *Proc. Natl. Acad. Sci. U. S. A.* **89,** 3135–3139
38. Wang, J., Yan, Y., Garrett, T. P. J., Liu, J.-H., Rodgers, D. W., Garlick, R. L., Tarr, G. E., Husain, Y., Reinherz, E. L., and Harrison, S. C. (1990) *Nature* **348,** 411–418
39. Golstein, P., Goridis, C., Schmitt-Verhulst, A.-M., Hayot, B., Pierres, A., van Agthoven, A., Kaufmann, Y., Eshhar, Z., and Pierres, M. (1982) *Immunol. Rev.* **68,** 5–42
40. Tomonari, K., and Spencer, S. (1990) *Int. Immunol.* **2,** 1189–1194
41. Leahy, D. J. (1995) *FASEB J.* **9,** 17–25
42. Johnson, I. D., Kang, H. C., and Haugland, R. P. (1991) *Anal. Biochem.* **198,** 228–237
43. Casabo, L. G., Mamalaki, C., Kioussis, D., and Zamoyska, R. (1994) *J. Immunol.* **152,** 397–404
44. Piller, F., Piller, V., Fox, R. I., and Fukuda, M. (1988) *J. Biol. Chem.* **263,** 15146–15150
45. Pascale, M. C., Erra, M. C., Malagolini, N., Serafini-Cessi, F., Leone, A., and Bonatti, S. (1992) *J. Biol. Chem.* **267,** 25196–25201
46. Garcia, K. C., Scott, C. A., Brunmark, A., Carbone, F. R., Peterson, P. A., Wilson, I. A., and Teyton, L. (1996) *Nature* **384,** 577–581
47. Renard, V., Delon, J., Luescher, I. F., Malissen, B., Vivier, E., and Trautmann, A. (1996) *Eur. J. Immunol.* **26,** 2999–3007
48. Wheeler, C. J., Chen, Y. F., Potter, T. A., and Parnes, J. R. (1998) *J. Immunol.* **160,** 4199–4207
49. Arden, B. (1998) *Curr. Opin. Immunol.* **10,** 74–81
50. Luescher, I. F., Vivier, E., Layer, A., Mahiou, J., Godeau, F., Malissen, B., and Romero, P. (1995) *Nature* **373,** 353–356

Expression, Purification, and Functional Analysis of Murine Ectodomain Fragments of CD8 αα and CD8αβ Dimers

Petra Kern, Rebecca E. Hussey, Rebecca Spoerl, Ellis L. Reinherz and Hsiu-Ching Chang

J. Biol. Chem. 1999, 274:27237-27243.
doi: 10.1074/jbc.274.38.27237